

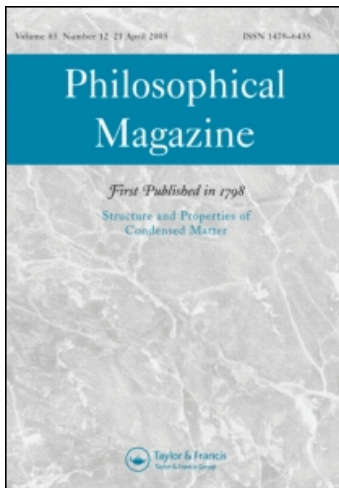
This article was downloaded by: [Brookhaven National Lab]

On: 19 May 2010

Access details: Access Details: [subscription number 921515202]

Publisher Taylor & Francis

Informa Ltd Registered in England and Wales Registered Number: 1072954 Registered office: Mortimer House, 37-41 Mortimer Street, London W1T 3JH, UK



Philosophical Magazine

Publication details, including instructions for authors and subscription information:
<http://www.informaworld.com/smpp/title~content=t713695589>

Electron-hole superlattices in GaAs/Al_xGa_{1-x}As multiple quantum wells

K. P. Walsh^{ab}; A. T. Fiory^b; N. M. Ravindra^b; D. R. Harshman^{cde}; J. D. Dow^e

^a US Army Energetics, Pyrotechnic Research and Technology, Picatinny, NJ 07806, USA ^b Department of Physics, New Jersey Institute of Technology, Newark, NJ 07102, USA ^c Physikon Research Corporation, Lynden, WA 98264, USA ^d Department of Physics, University of Notre Dame, Notre Dame, IN 46556, USA ^e Department of Physics, Arizona State University, Tempe, AZ 85287, USA

To cite this Article Walsh, K. P. , Fiory, A. T. , Ravindra, N. M. , Harshman, D. R. and Dow, J. D. (2006) 'Electron-hole superlattices in GaAs/Al_xGa_{1-x}As multiple quantum wells', *Philosophical Magazine*, 86: 23, 3581 – 3593

To link to this Article: DOI: 10.1080/14786430600677694

URL: <http://dx.doi.org/10.1080/14786430600677694>

PLEASE SCROLL DOWN FOR ARTICLE

Full terms and conditions of use: <http://www.informaworld.com/terms-and-conditions-of-access.pdf>

This article may be used for research, teaching and private study purposes. Any substantial or systematic reproduction, re-distribution, re-selling, loan or sub-licensing, systematic supply or distribution in any form to anyone is expressly forbidden.

The publisher does not give any warranty express or implied or make any representation that the contents will be complete or accurate or up to date. The accuracy of any instructions, formulae and drug doses should be independently verified with primary sources. The publisher shall not be liable for any loss, actions, claims, proceedings, demand or costs or damages whatsoever or howsoever caused arising directly or indirectly in connection with or arising out of the use of this material.

Electron–hole superlattices in GaAs/Al_xGa_{1–x}As multiple quantum wells

K. P. WALSH^{†‡}, A. T. FIORY[‡], N. M. RAVINDRA[‡],
D. R. HARSHMAN^{*¶§||} and J. D. DOW^{||}

[†]US Army Energetics, Pyrotechnic Research and Technology, Picatinny, NJ 07806, USA

[‡]Department of Physics, New Jersey Institute of Technology, Newark, NJ 07102, USA

[§]Physikon Research Corporation, P.O. Box 1014, Lynden, WA 98264, USA

[¶]Department of Physics, University of Notre Dame, Notre Dame, IN 46556, USA

^{||}Department of Physics, Arizona State University, Tempe, AZ 85287, USA

(Received 24 January 2006; in final form 8 March 2006)

A GaAs/Al_xGa_{1–x}As semiconductor structure is proposed, which is predicted to superconduct at $T_c \approx 2$ K. Formation of an alternating sequence of electron- and hole-populated quantum wells (an electron–hole superlattice) in a modulation-doped GaAs/Al_xGa_{1–x}As superlattice is considered. This superlattice may be analogous to the layered electronic structure of high- T_c superconductors. In the structures of interest, the mean spacing between nearest electron (or hole) wells is the same as the mean distance between the electrons (or holes) in any given well. This geometrical relationship mimics a prominent property of optimally doped high- T_c superconductors. Band bending by built-in electric fields from ionized donors and acceptors induces electron and heavy-hole bound states in alternate GaAs quantum wells. A proposed superlattice structure meeting this criterion for superconductivity is studied by self-consistent numerical simulation.

1. Introduction

The stoichiometry and quasi two-dimensional layered geometry of high- T_c superconducting materials can be optimized both for T_c and for the bulk Meissner fraction, as first noted by Harshman and Mills [1]. The superconductivity was also shown to be electronic in origin, since T_c scales with the Fermi energy in two dimensions, rather than with the Debye phonon energy as in conventional superconductivity. Furthermore, these optimal T_c and Meissner fraction materials obey certain criteria relating the geometry to the electronic properties. Of particular relevance to the present study is the parameter, $\beta = Nd^2$, that characterizes the sheet hole density, N , and the layer spacing, d . For optimized high- T_c superconductors, β approaches unity, a criterion that specifies that the average spacing between superconducting carriers tends to be equal to the spacing between superconducting layers. These authors also suggested that high- T_c -like superconductivity occurs in GaAs/Al_xGa_{1–x}As heterostructures composed of multiple quantum wells of either

*Corresponding author. Email: drh@physikon.net

electrons or holes (one type of carrier, not both). To properly synthesize the electronic structure of high- T_c superconductors, one of the authors of this paper (DRH) more recently proposed that both electron and hole layers need to be included. This has led us to develop a superconductor model with alternating layers of electrons and holes (an electron-hole superlattice). In this communication, we propose an electron-hole superlattice in a GaAs/ $\text{Al}_x\text{Ga}_{1-x}\text{As}$ superlattice structure that meets the criterion of $Nd^2 \approx 1$ ($\beta \approx 1$). Its properties have been determined by self-consistent numerical simulation.

Superconducting transition temperatures are estimated from the expression [2]:

$$kT_c = 0.25 \hbar \Omega [\exp(2/\Lambda) - 1]^{-1/2} \quad (1)$$

with $\hbar\Omega$ being the Fermi energy in two dimensions. Equation (1) is a generalization to strong coupling ($\Lambda \sim 2-3$) of the theoretical analysis presented in [1] and is consistent with experiments on high- T_c superconductors [3].

The electron-hole superlattice proposed in this study has equal sheet concentrations of mobile electrons and holes, $N_e = N$ and $N_h = N$, respectively, that occupy separate and alternating GaAs quantum well layers and are repeated with spatial periodicity d (see figure 1) [4, 5].

Electrostatic fields created by fixed ionized donor and acceptor layers induce band bending and bound states of energies (quasi-Fermi energies) for electrons and holes of E_e and E_h , respectively. The ionized impurity layers, which produce an

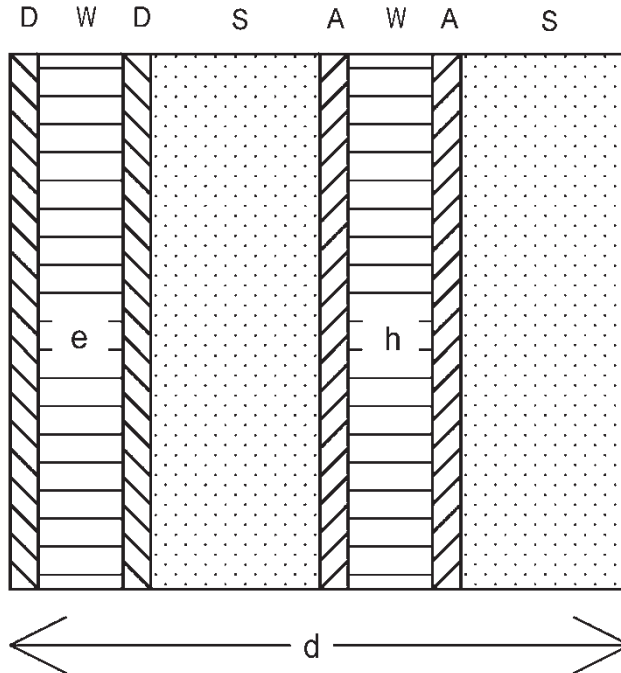


Figure 1. Schematic of a superlattice period of width d . GaAs quantum wells (W) contain electrons (e) or holes (h). $\text{Al}_x\text{Ga}_{1-x}\text{As}$ layers are donor doped (D), acceptor doped (A), or undoped spacers (S).

electrostatic energy per superlattice period comparable to twice the band gap of GaAs, correspond to the ionic background in high- T_c crystals. The energy relevant to superconductivity, in analogy to the high- T_c case, involves only the mobile charges in the quantum wells. This is modelled using equation (1) in terms of the bound states in one superlattice period, for which $\hbar\Omega = E_e + E_h$.

Coulomb interactions among the mobile charges in multiple quantum well systems are characterized by two dimensionless parameters, $r_s = (a_B^*)^{-1} (\pi N)^{-1/2}$, where a_B^* is the Bohr radius of either electrons or holes, and $\gamma = 2r_s a_B^*/d$. The parameter r_s is determined by the ratio of the Coulomb interaction energy to the kinetic energy within a quantum well. The parameter γ is determined by the ratio of intrawell and interwell Coulomb energies, and can be written as $\gamma = 2(\pi N d^2)^{-1/2} = 2(\pi\beta)^{-1/2}$. Since the idea of synthesizing a high- T_c superconductor in a semiconductor is tested here, one has $\beta = 1$ or $\gamma = 1.13$. The regime of high- T_c superconductivity, therefore, corresponds to moderate interlayer coupling (defined as $\gamma \approx 1$).

The application being simulated is the epitaxial growth of the superlattice on the (311)A plane of GaAs [6] for which the electron and heavy-hole effective masses are $m_e^* = 0.067m_0$ and $m_h^* = 0.15m_0$ [7], respectively, where m_0 is the electron rest mass. Tunneling splitting of the electron and hole sub-bands is so small in the proposed structure that it may be neglected. Charge transport is not of the same magnitude in the negatively and positively charged GaAs quantum wells owing to the different effective masses and mobilities of electrons and holes. This asymmetry between electrons and holes provides a mechanism for superconductivity mediated by Coulomb interactions as given by equation (1). The energies E_e and E_h and the parameter γ are determined by self-consistent numerical solutions of the Schrödinger and Poisson equations at $\beta = 1$ and for the structure of figure 1. Sensitivities to modulation doping, barrier heights, quantum well structure and temperature, as well as issues of feasibility, are examined in the following sections.

2. Electron–hole superlattices in GaAs/Al_xGa_{1-x}As

The proposed superlattice structure comprises multiple repeating undoped GaAs and doped or undoped Al_xGa_{1-x}As layers described for one period in table 1 and illustrated schematically in figure 1. Charge transfer and band bending to form equilibrium electron–hole superlattices in such structures have been determined by numerical analysis.

2.1. Design considerations

The superlattice has multiple GaAs quantum well layers (W) each of thickness d_w . On either side of each GaAs well are Al_xGa_{1-x}As layers of thickness d_s that are alternately doped with donors (D) to form electron wells (e) or with acceptors (A) to form hole wells (h). The volume densities of donors and acceptors are denoted by n_D and n_A , respectively, and the corresponding calculated sheet densities of the dopants

Table 1. Layer structure of one period in a GaAs/Al_xGa_{1-x}As superlattice of alternating electron and hole GaAs quantum wells produced by modulation doping. The width of a superlattice period is $d = 2(d_W + d_S + 2d_\delta)$, where d_W , d_S and d_δ symbolize thickness of quantum wells, spacers and doped layers, respectively. Layer type designations are D for donor, A for acceptor, W for quantum well and S for spacer. N_D and N_A denote donor and acceptor impurity sheet densities, respectively; N_e and N_h denote electron and hole carrier sheet densities in the quantum wells, respectively.

Layer	Type	Composition	Description	Thickness
1	D	Al _x Ga _{1-x} As	Donor doped, N_D	d_δ
2	W	GaAs	Electron well, N_e	d_W
3	D	Al _x Ga _{1-x} As	Donor doped, N_D	d_δ
4	S	Al _x Ga _{1-x} As	Undoped spacer	d_S
5	A	Al _x Ga _{1-x} As	Acceptor doped, N_A	d_δ
6	W	GaAs	Hole well, N_h	d_W
7	A	Al _x Ga _{1-x} As	Acceptor doped, N_A	d_δ
8	S	Al _x Ga _{1-x} As	Undoped spacer	d_S

are $N_D = d_\delta n_D$ and $N_A = d_\delta n_A$, respectively. Charge neutrality in a finite superlattice requires equal total numbers of donors and acceptors. The doped layers and quantum wells are adjacent to one another in the simulated structure. However, undoped Al_xGa_{1-x}As spacers between the doped layers and the quantum wells can be introduced to reduce scattering by ionized dopants and to boost mobilities, thus ensuring metallic conduction at low temperature [8]. Undoped Al_xGa_{1-x}As spacer layers (S) of thickness d_S separate the donor- and acceptor-doped Al_xGa_{1-x}As layers.

The objective of the numerical simulation is to find structures in which the GaAs quantum wells are alternately occupied in thermal equilibrium by electrons and holes of sheet carrier densities, N_e and N_h , respectively. The layers must also satisfy the $\beta \approx 1$ criterion, expressed as $N_e = N_h \approx d^{-2}$. The length d is the superlattice period, which is given in terms of the layer thicknesses (see table 1) as:

$$d = 2(d_W + d_S + 2d_\delta) \quad (2)$$

In equilibrium, electrons are transferred from the donors to the acceptors, creating a modulated built-in electric field, $F(y)$, where y is the coordinate in the direction normal to the layers. The field is produced in most part by ionization of donors and acceptors in the d_δ -Al_xGa_{1-x}As layers of sheet concentrations, N_D^+ and N_A^- , respectively ($N_D^+ \approx N_D$ and $N_A^- \approx N_A$). Contributions to $F(y)$ from charges in the quantum wells are a comparatively small perturbation, since simulation shows that $N_e \ll N_D^+$ and $N_h \ll N_A^-$ for $\beta \sim 1$. At full ionization (low temperatures), the magnitude of $F(y)$ attains a maximum in the undoped spacer layers, given by

$$F_0 = 4\pi e N_D / \epsilon_x = 4\pi e N_A / \epsilon_x \quad (3)$$

where ϵ_x is the dielectric constant of Al_xGa_{1-x}As. At low temperatures and for small impurity concentrations N_D and N_A , charge is transferred from the donors to the acceptors, but the Fermi level lies within the GaAs gap and the quantum wells remain unoccupied. At a threshold impurity concentration, N_{th} , the build-in electric

field is sufficient to move the Fermi level into the conduction and valence bands of alternate GaAs wells, and bound states are formed. At threshold, the maximum built-in electric field approximates E_g/ed_S , where E_g is the band gap of GaAs, and this leads to

$$F_0 \approx E_g/ed_S. \quad (4)$$

The threshold doping concentration is, thus, estimated as,

$$N_{\text{th}} \approx \varepsilon_x E_g / 4\pi ed_S. \quad (5)$$

For doping concentrations exceeding N_{th} , excess free charge spills over into the GaAs quantum wells, which become populated by two-dimensional electron or hole gases of sheet densities N_e and N_h , and energy eigenvalues of $E_e = \pi\hbar^2 N_e / m_e^{**}$ and $E_h = \pi\hbar^2 N_h / m_h^{**}$, respectively. Here, the effective masses, m_e^{**} and m_h^{**} , are the electron and hole effective masses of GaAs, modified by the quantum confinement and the wave function extension into the $\text{Al}_x\text{Ga}_{1-x}\text{As}$ barriers. Numerical simulation is used to determine N_{th} , N_e , N_h , E_e and E_h self-consistently in multiple quantum wells.

Since T_c scales with Fermi energy, which is proportional to N in two dimensions, maximizing T_c implies selecting the largest possible sheet carrier densities of electrons and holes that is consistent with also satisfying the criteria $Nd^2 = 1$. Thus, T_c scales with d^{-2} and maximizing T_c corresponds with minimizing d . Materials properties, primarily the internal dielectric strength of the undoped $\text{Al}_x\text{Ga}_{1-x}\text{As}$ spacer layer, impose a practical upper limit on the built-in electric field, which is denoted as F_{max} . Thus, the constraint $F_0 \leq F_{\text{max}}$, becomes equivalent to a constraint on the spacer width, expressed as $d_S \geq E_g / eF_{\text{max}}$. A minimum spacer width in turn imposes a minimum allowable length for the superlattice period, expressed as $d > d_{\text{min}}$, where

$$d_{\text{min}} = 2(E_g / eF_{\text{max}} + d_w + 2d_s). \quad (6)$$

Approaches for minimizing d_{min} in electron–hole superlattices are discussed in the next section for the design of a superlattice test structure.

2.2. Superlattice structure

The proposed composition of superlattices in $\text{GaAs}/\text{Al}_x\text{Ga}_{1-x}\text{As}$ is based on the eight-layer sequence in one superlattice period as listed in table 1. The sequence of layers in one period is written with the notation, (D, W, D, S, A, W, A, S), where symbols denote the four layer types: donor, D; quantum well, W; spacer, S; and acceptor, A. This entire layer sequence is denoted by shorthand symbol, P. Multiply repeating the sequence, (P, P, ..., P), produces a structure that begins as n-type and ends as p-type. To make the structure centro-symmetric with zero net dipole moment, we insert fractional-period layers at the ends. At the beginning, we insert a quarter period that is n-type, (S, W, D), a spacer layer, S, and a half period that is p-type, (A, W, A, S); and, at the end, a quarter period that is n-type, (D, W, S). The superlattice structure is enclosed by undoped $\text{Al}_x\text{Ga}_{1-x}\text{As}$ substrate and capping layers, which are simulated by layers of thickness d_C and denoted by the symbol, C.

Thus, the layer sequence in the simulated structure (retaining the parentheses for illustration) is,

$$(C), (S, W, D), S, (A, W, A, S), (P, P, \dots, P), (D, W, S), (C) \quad (7)$$

The prescription for the layer sequence given in expression (7) produces a finite superlattice structure with the quantum well sequence e–h–...–h–e (e: electron well; h: hole well) that is mirror symmetric with respect to the midpoint. The quarter periods at the ends provide smooth transitions for terminating the superlattice at the capping layers. For an N -period superlattice, this method produces carrier concentrations, N_e and N_h , for the $N-3$ electron and hole wells in the middle portion of the superlattice that are insensitive to boundary effects (This was verified by varying the number of periods by a factor of three and varying the thickness of the capping layers by a factor of two).

The construction of an h–e–...–e–h superlattice is as in expression (7), except that D and A are interchanged (dopant types interchanged). Simulations of superlattices of types e–h–...–h–e and h–e–...–e–h yield results for N_e and N_h that are the same to within 0.1%.

Optimal selections of the layer thicknesses, which are given symbolically in table 1, are based on the goal of making the minimum superlattice period given in equation (6), d_{\min} , as small as possible so that N and, thus, T_c , can be as large as possible. For a given E_g/eF_{\max} , superlattices with all layers spacings equal, i.e. $d_\delta = d_W = d_S$, require a larger d_{\min} than a non-uniform scheme where d_S is maximized at the expense of smaller d_δ and d_W . The width of the doping layers, d_δ , can be minimized to effectively a monolayer in epitaxial film growth (i.e. delta doping) [6, 9]. However, the width of the quantum wells, d_W , cannot be made arbitrarily narrow, because it is necessary that occupied electron and hole eigenstates form at low temperature ($E_e > k_B T_c$, $E_h > k_B T_c$). Increasing the Al concentration in $\text{Al}_x\text{Ga}_{1-x}\text{As}$ helps to reduce d_W by increasing the barrier height for quantum confinement. We considered an Al alloy composition maximum of $x \approx 0.4$ to avoid band crossover near $x \sim 0.45$ in $\text{Al}_x\text{Ga}_{1-x}\text{As}$ that complicates the analysis. In testing the structure of expression (7), we assume that a maximum built-in field of $F_{\max} = 5 \times 10^5 \text{ V/cm}$ can be realized in semi-insulating $\text{Al}_x\text{Ga}_{1-x}\text{As}$ dielectrics [10]. While this value is about five times larger than typically employed in bilayer studies [11], the electron–hole superlattice proposed in this study should be stable against dielectric breakdown because the field lines terminate inside the structure and the surface charge density can be zero.

2.3. Numerical simulation

Solutions for the carrier densities and eigenstates in the quantum wells at various temperatures were obtained by self-consistent numerical simulations using the one-dimensional Schrödinger–Poisson solver developed by Snider [12]. Simulations are needed to determine doping levels, owing to tunneling between wells through the $\text{Al}_x\text{Ga}_{1-x}\text{As}$ barriers. Finite temperature also influences dopant ionization and effective barrier heights. Our procedure calculates mobile charge concentrations using Boltzmann statistics. Fermi levels are obtained by inversion of integrals over

Fermi–Dirac functions [12]. In the simulation, the bending of the conduction and valence bands, electron and hole concentrations, internal field distributions, and quantum well wavefunctions are calculated as a function of the depth coordinate, y .

Superlattices were modelled with a finite element numerical method [13] using a discrete mesh in the depth coordinate, dy , that was varied from 0.01 to 0.1 nm to examine sensitivity of results to the magnitude of dy . Energy eigenvalues were found for bound quantum well states that form two-dimensional electron or hole gases. The thickness of the capping layers is taken to be sufficiently large that the amplitudes of the bound-state wavefunctions at the surface and substrate are negligibly small, which is possible because our proposed symmetric device structure has zero bias and zero net charge. Capping layers $d_C = 10$ nm are found to be of sufficient thickness to allow one to impose zero wavefunction slope as the boundary condition.

Simulations were performed for various thicknesses of the layers in the structure, and for various dy , doping concentrations, N_D and N_A ($N_D = N_A$), and temperatures, T . In keeping the layer thicknesses fixed and varying the doping concentration, there is a threshold doping concentration for the onset of well population. Holes are found to be formed first, owing to $m_h^* > m_e^*$, and they populate the GaAs wells surrounded by acceptor-doped $\text{Al}_x\text{Ga}_{1-x}\text{As}$. The formation of electrons flowing into the GaAs wells surrounded by donor-doped $\text{Al}_x\text{Ga}_{1-x}\text{As}$ occurs at a slightly larger doping level. The electron clouds surrounding these GaAs wells screen the positive charge of the holes, which facilitates the formation of alternating electron and hole layers.

2.4. Electron–hole superlattice results

In testing superlattice structures by simulations, we studied models with both uniform and non-uniform layer spacings. We present here the results for N_e and N_h that were obtained with non-uniform spacings, as these can be optimized for the smallest allowable superlattice period, subject to the constraint on the built-in field, $F_0 \leq F_{\max}$. Quantum well widths, d_W , from 5 to 20 nm were studied. The built-in field is an increasing function of d_W (while keeping the superlattice period fixed), whereas the efficiency of charge transfer, η , defined as the fraction of charge transferred from the dopants to the quantum wells, is a decreasing function of d_W . We find that $d_W = 10$ nm is suitable for simultaneously satisfying the conditions of low F_0 and high η . Doped layer thicknesses, d_δ , in the range of 0.5 to 10 nm were studied. Equation (2) shows that, for a given superlattice period d , reducing d_δ allows one to increase spacer thickness d_S and, as expected from equation (4), to reduce the peak internal fields. A superlattice period of $d = 80$ nm was thus determined from d_{\min} using equation (6), where $F_{\max} = 5 \times 10^5$ V/cm, $d_W = 10$ nm and $d_\delta \sim 0.5$ nm.

Results for sheet carrier concentrations, N_e and N_h , were obtained in a range of alloy concentrations $0.15 \leq x \leq 0.45$. The doping concentration needed to produce a given carrier concentration decreases by 2.5% per 0.1 incremental increase in x . Varying x simultaneously with the doping concentration so as to yield a given carrier concentration was found to produce superlattices with otherwise almost identical properties. The results for N_e and N_h that were obtained at zero temperature for

Table 2. Layer thickness and doping specifications for a modulation doped GaAs/ $\text{Al}_{0.4}\text{Ga}_{0.6}\text{As}$ superlattice of electrons and holes at zero temperature ($\beta = N_c d^2 = N_h d^2 = 1$).

Description	Symbol	Value
Superlattice period	d	80.0 nm
Quantum wells width	d_W	10.0 nm
Doped layer width	d_δ	3.0 nm
Undoped spacer width	d_S	24.0 nm
Volume doping concentration	n_D, n_A	$1.23 \times 10^{19} \text{ cm}^{-3}$
Sheet doping concentration	N_D, N_A	$3.68 \times 10^{12} \text{ cm}^{-2}$
Sheet electron, hole concentration	N_e, N_h	$1.56 \times 10^{10} \text{ cm}^{-2}$
Geometric parameter	β	1

$x=0.4$ are presented in table 2, corresponding to which the simulation procedure readily finds the bound-state wavefunctions.

The $\beta=1$ criterion applied to a superlattice of periodicity $d=80$ nm requires that the electron and hole concentrations each be $1.56 \times 10^{10} \text{ cm}^{-2}$. This carrier density substantially exceeds the minimum requirement ($N \sim 3 \times 10^9 \text{ cm}^{-2}$) for metallic behaviour in GaAs quantum wells [8], which is a pre-requisite for superconductivity. Simulations yield results for the electron and hole concentrations that are within 1% of this value for donor and acceptor concentrations of $N_D = N_A = 3.68 \times 10^{12} \text{ cm}^{-2}$, and thus $\gamma = 1.13$ is derived self-consistently. Figures 2–4 present some of the results obtained at $T=0$.

Figure 2 shows the modulation of the conduction and valence band edges, E_C and E_V , for a superlattice of periodicity $d=80$ nm as functions of the depth coordinate, y . The zero of energy is the Fermi level, which is constant. The solid curve corresponds to the monolayer doping approximation, $d_\delta=0.5$ nm, and the dotted points correspond to $d_\delta=3.0$ nm. The effect of varying d_δ over this range is noticed mainly as slight changes in the undoped regions near the quantum wells. For this simulation, the Fermi level lies at 51 meV above the conduction band edge in the electron quantum wells and at 23 meV below the valence band edge in the hole quantum wells. Band edges within the quantum wells vary by ± 0.19 and ± 0.18 meV for electrons and holes, respectively, owing to band bending by bound-state charges. The mean conduction band edge in the electron wells decreases by 0.28 meV per 10^{10} cm^{-2} incremental increase in N_D , and the mean valence band edge in the hole wells increases by 0.13 meV per 10^{10} cm^{-2} incremental increase in N_A .

The energy eigenvalues of the bound electron and hole states are $E_e = 0.56$ meV and $E_h = 0.25$ meV. This yields $\hbar\Omega = 0.81$ meV and from equation (1) with $\Lambda \sim 2-3$, $T_c \sim 1.8-2.4$ K. The results for E_e and E_h correspond to quantum-confined effective masses (m^{**}) that are only about 1% less than bulk GaAs effective masses (m^*).

Figure 3 shows the built-in electric field $F(y)$ as a function of depth coordinate y for the same simulation results that are presented in figure 2. The magnitude of the field is maximum and nearly constant in the spacer layers, and is of amplitude F_0 as estimated in equation (4). The built-in field is smallest, $F_0 \approx 500$ kV/cm, for simulated monolayer doping ($d_\delta=0.5$ nm) where the undoped spacers can be the widest ($d_S=290$ nm) as determined from equation (2) for well thickness $d_W=10$ nm and periodicity $d=80$ nm.

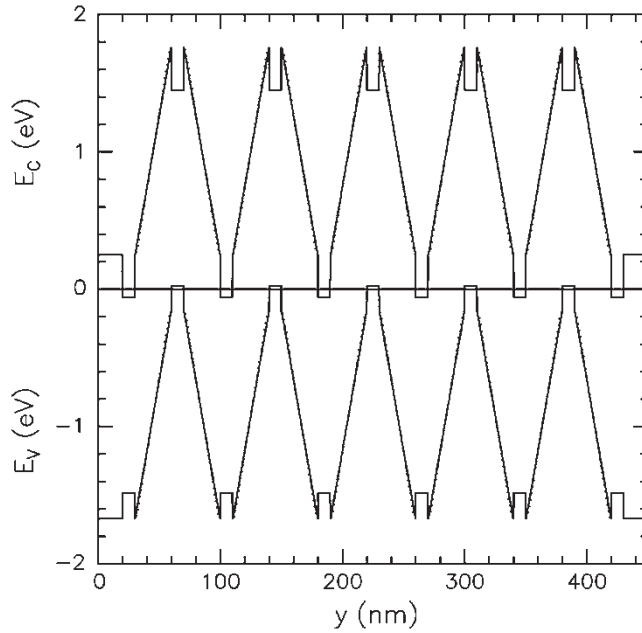


Figure 2. Edges of conduction, E_c , and valence, E_v , bands for modulation doped electron-hole GaAs/Al_{0.4}Ga_{0.6}As superlattices (80 nm period) as functions of depth, y . Widths of doped layers (d_δ) are 0.5 nm (solid curves) and 3.0 nm (dotted curves). Zero of energy is the Fermi level. Quantum wells of width $d_w = 10$ nm are occupied by electrons where $E_c < 0$ and by holes where $E_v > 0$.

The variations of electron and hole concentrations N_e and N_h with $N_D = N_A$ are shown in figure 4. Extrapolations of N_e and N_h to zero give the threshold doping level, $N_{th} = 3.67 \times 10^{10} \text{ cm}^{-2}$, which is about 10% less than the estimate obtained from equation (5). The results in figure 4 can be expressed as the functions, $N_e = \alpha_e(N_D - N_{D,th})$ and $N_h = \alpha_h(N_A - N_{A,th})$ for the electron and hole densities, respectively. The intercepts for donor doping, $N_{D,th} \approx N_{th}$, and acceptor doping, $N_{A,th} \approx N_{th}$, are nearly the same (see figure 4). The slopes are also approximately equal $\alpha_e \approx \alpha$ and $\alpha_h \approx \alpha$, where $\alpha = 1.3$ defines sensitivity of changes in carrier concentration to changes in doping concentration. Sensitivity coefficients α are found to be nearly independent of x . The efficiency of charge transfer to the quantum wells, calculated as $\eta = N_e/N_D^+$ for the electrons or N_h/N_A^- for the holes, is about $\eta = 0.43\%$ for superlattices satisfying the criterion $\beta = 1$. We find that η increases with x , increasing by 8% over the range $x = 0.15$ – 0.45 , owing to increased barrier heights at the GaAs/Al _{x} Ga _{$1-x$} As interfaces.

Figure 5 shows the variation of sheet carrier concentration, $N_e \approx N_h$, with temperature for a superlattice with doping layers of thickness $d_\delta = 3$ nm. There is a small variation in carrier concentration in the region $T < 2$ K, owing to thermal effects in ionization and charge transfer. The simulations, thus, show that the equilibrium carrier concentrations can be taken as nearly independent of temperature in the region where the superconductive condensate is expected to exist, for $T_c \sim 2$ K.

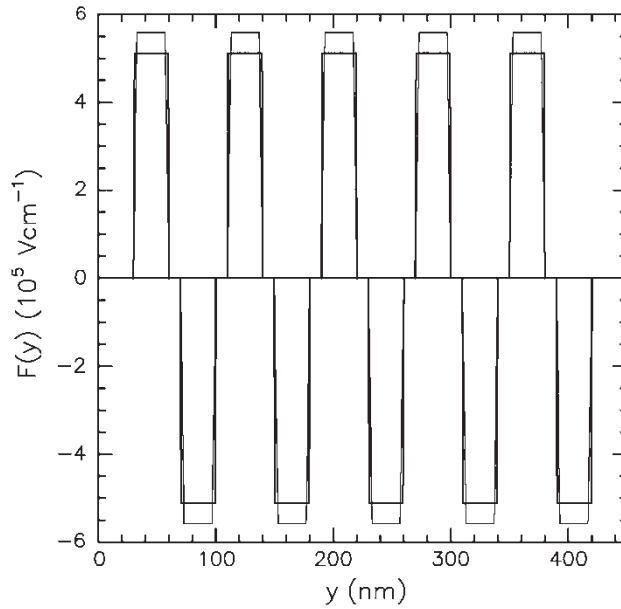


Figure 3. Variation of the built-in electric fields, $F(y)$, of modulation doped electron-hole GaAs/ $\text{Al}_{0.4}\text{Ga}_{0.6}\text{As}$ superlattices as functions of depth, y . Widths of doped layers (d_δ) are 0.5 nm (thick curves) and 3.0 nm (thin curves). Maximum field strength occurs in the undoped $\text{Al}_{0.4}\text{Ga}_{0.6}\text{As}$ spacer layers.

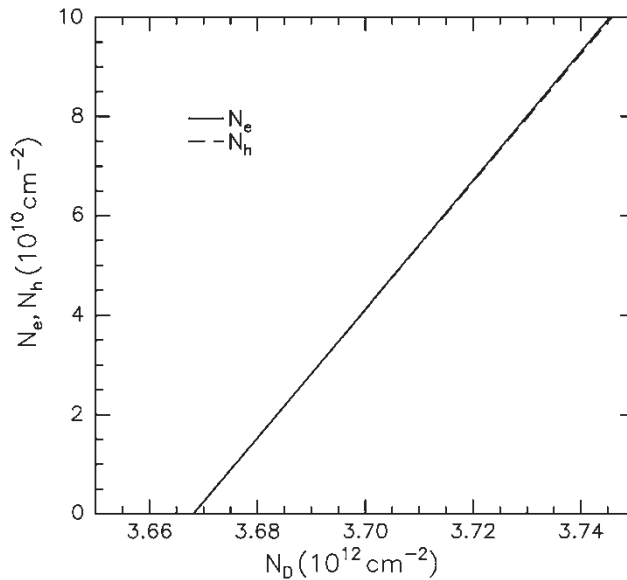


Figure 4. Variation of sheet electron and hole densities, N_e and N_h , respectively, with sheet concentration of dopants ($N_D = N_A$) in modulation doped layers (of thickness $d_\delta = 3$ nm) of a GaAs/ $\text{Al}_{0.4}\text{Ga}_{0.6}\text{As}$ superlattice with GaAs quantum wells of thickness $d_w = 10$ nm and periodicity $d = 80$ nm.

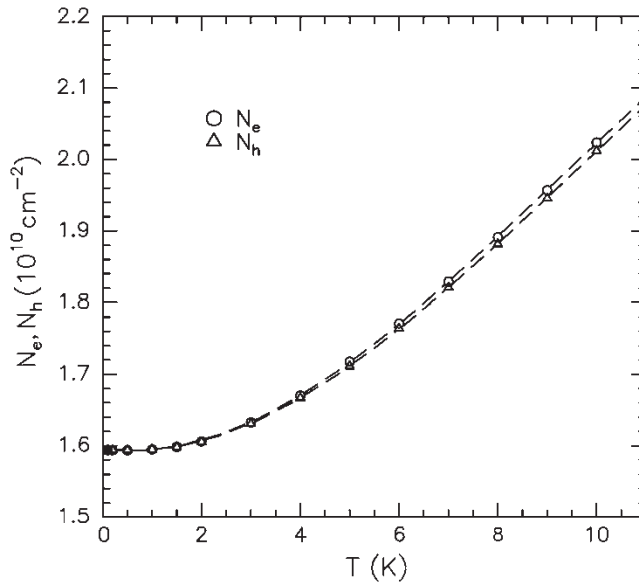


Figure 5. Temperature dependence of sheet electron (circles) and hole (triangles) densities calculated for a modulation doped (impurity concentration: $3.68 \times 10^{12} \text{ cm}^{-2}$; doped layer thickness: 3 nm) GaAs/ $\text{Al}_{0.4}\text{Ga}_{0.6}\text{As}$ superlattice with GaAs quantum wells of thickness 10 nm and periodicity 80 nm. (Dashed curves are guides to the eye).

3. Discussion

The above results illustrate that producing a superlattice of electrons and holes in GaAs/ $\text{Al}_x\text{Ga}_{1-x}\text{As}$ heterostructures is feasible and specific results were obtained for an assumed built-in electric field $F_{\text{max}} = 5 \times 10^5 \text{ V/cm}$. While the fabrication of such a superlattice may be technically challenging, we assume that any given layer's width can be controlled to an accuracy of 0.5 nm and that doping concentrations can be controlled to an accuracy of 0.1%. Variations during growth of the superlattice, such as fluctuations in the spacing of any layer, will lead to 2% variations in superlattice period. The fluctuations in the sheet concentration of the dopants will be 0.14%. Variations in carrier concentrations N will be larger than variations in dopant concentrations N_D or N_A by a factor $\alpha/\eta \approx 300$, which is the ratio of sensitivity parameter α and the efficiency coefficient η , so that the variation in N due to doping fluctuations is estimated to be 30%. This shows that fluctuations in $\beta = Nd^2$ are expected to be dominated by fluctuations in doping, since fluctuations in d^2 are comparatively smaller at 4%. Taking into account the variation of T_c in high- T_c superconductors at optimal doping [1], the superconducting transition is expected to be inhomogeneously broadened by 2% for such growth fluctuations.

Simulations were also performed to determine the consequences of growing a superlattice with either defective doping or a defective width in one of the layers. These were examined by changing the thickness or doping concentration of a doped layer in the simulated superlattice. The perturbations produced by such defects are

changes in N_e or N_h that are localized in the quantum well closest to the defective layer.

Semiconductor systems with large dielectric constants and band gaps (e.g. such as structures based on GaN) can tolerate larger internal fields before breaking down. Choosing a semiconductor material with dielectric strength higher than that of AlGaAs and GaAs would theoretically increase the dopant concentration N , decrease d and increase T_c , since the built-in electric field can be higher.

4. Conclusions

The feasibility of forming superconducting electron–hole superlattices in modulation-doped GaAs/Al_xGa_{1-x}As heterostructures was examined by a self-consistent numerical solution of the Schrödinger and Poisson equations. These superlattices emulate the electronic structure of high- T_c superconductors, $Nd^2 \approx 1$, where N is the sheet carrier density in the layers and d is the superlattice period. Results are based on a maximum built-in electrostatic field of 500 kV/cm, which dictates a minimum superlattice period of $d = 80$ nm. The corresponding sheet carrier density of electrons and holes is $N = 1.56 \times 10^{10} \text{ cm}^{-2}$. Based on a strong-coupling electronic model of superconductivity, we believe that a superconductor with a transition temperature of 2 K will result from such an electron–hole superlattice.

Acknowledgements

This work was supported in part by US Army Energetics, the US Army Research Office (W911NF-05-1-0346 ARO), the US Air Force Office of Scientific Research, Physikon Research Corporation (PL-206) and New Jersey Institute of Technology. The authors are most grateful for this support.

References

- [1] D.R. Harshman and A.P. Mills, *Phys. Rev. B* **45** 10684 (1992).
- [2] J.C. Phillips, *Physics of High- T_c Superconductors* (Academic Press, San Diego, 1989).
- [3] D.R. Harshman, W.J. Kossler, X. Wan, *et al.*, *Phys. Rev. B* **69** 174505 (2004).
- [4] The structure we consider bears some resemblance to $n-i-p-i$ (n : donor, i : semi-insulating, p : acceptor) superlattices for other applications, e.g. Stark effect devices [K.-K. Law, *et al.*, *Optics Lett.* **14** 230 (1989); G.W. Yoffe, *et al.*, *IEEE Trans. Electron. Devices* **40** 2144 (1993)]; non-linear optics [G. Li, *et al.*, *Appl. Phys. Lett.* **69** 4218 (1996)]; and THz photomixers [F. Renner, *et al.*, *Phys. Status Solidi (a)* **202** 965 (2005)].
- [5] Electron and hole gases have also been manipulated by optical excitation [U.D. Kiel, *et al.*, *Phys. Rev. B* **44** 13504 (1991)] and with Ohmic contacts [B.E. Kane, *et al.*, *Appl. Phys. Lett.* **65** 3266 (1994)].

- [6] G. Li, C. Jagadish, M.B. Johnston, *et al.*, Appl. Phys. Lett. **69** 4218 (1996); C. Jagadish, G. Li, M.B. Johnston, *et al.*, Sci. Eng. B **51** 103 (1998).
- [7] B.E. Cole, J.M. Chamberlain, M. Henini, *et al.*, Phys. Rev. B **55** 2503 (1997).
- [8] A.P. Mills Jr, A.P. Ramirez, L.N. Pfeiffer, *et al.*, Phys. Rev. Lett. **83** 2805 (1999).
- [9] S.J. Papadakis, E.P. De Poortere and M. Shayegan, Phys. Rev. B **62** 15375 (2000).
- [10] Electronics Archive (Ioffe Physics–Technical Institute, St. Petersburg, Russian Federation). Available online at: <http://www.ioffe.ru/SVA/NSM/Semicond/AlGaAs/ebasic.html> (accessed 12 September 2005).
- [11] S. Brand and R.A. Abram, J. Phys. C: Solid State Phys. **16** 6111 (1983); W. Batty and D.W.E. Allsopp, IEEE Photonics Tech. Lett. **7** 635 (1995); C.V.-B. Tribuzy, M.C.L. Areiza, S.M. Landi, *et al.*, Appl. Phys. Lett. **86** 23501 (2005).
- [12] G.L. Snider, I.-H. Tan and E.L. Hu, J. Appl. Phys. **68** 2849, (1990); I.-H. Tan, G.L. Snider and E.L. Hu, J. Appl. Phys. **68** 4071(1990); G. Snider, *1D Poisson/Schrödinger User's Manual: A Band Diagram Calculator* (University of Notre Dame Press, Notre Dame, Indiana). Available online at: <http://www.nd.edu/~gsnider> (accessed 2 June 2005).
- [13] L.R. Ram-Mohan, *Finite Element and Boundary Element Applications in Quantum Mechanics* (Oxford University Press, 2002), pp. 241–256.